

Optimal Resource Allocation for Multi-user Video Streaming over mmWave Networks

Zhifeng He and Shiwen Mao

Department of Electrical and Computer Engineering

Auburn University, Auburn, AL 36849-5201 USA

Email: zzh0008@tigermail.auburn.edu, smao@ieee.org

Abstract—We investigate the resource allocation problem, including time slot allocation, channel allocation, and power adaptation, in a millimeter Wave (mmWave) network with multiple transmission links, multiple channels, and a PicoNet Coordinator (PNC). Each link has a video session to transmit from the transmitter to the receiver. The objective is to minimize the number of time slots to finish the video sessions of all links by jointly optimizing channel allocation and time slot allocation for links, while considering the possible interference between different links on the same channel. The optimal solution for the formulated problem is computationally prohibitive to obtain due to the exponential complexity. We developed a column generation based method to reformulate the original problem into a main problem along with a series of sub-problems, with greatly reduced complexity. We prove that the optimal solution for the reformulated problem converges to the optimal solution of the original problem, and we derived a lower bound for the performance of the reformulated problem at each iteration, which will finally converge to the global optimal solution. The proposed scheme is validated with simulations with its superior performance over existing work is observed.

Keywords—5G wireless; column generation; multi-user video streaming; mmWave communications; resource allocation.

I. INTRODUCTION

Recently, millimeter wave (mmWave) communications has attracted intense interest in the research community. mmWave communications is a promising technique to become the core technology for future 5G wireless systems due to the huge spectrum that is available. Thus it has a great potential to satisfy the fast growing demand on wireless network capacity. Significant efforts has been made on developing mmWave communications and networking technologies and standardization recently.

However, there are still many challenging problems that need to be addressed to fully harvest the potential of mmWave communications. The wireless signal attenuation in 60 GHz channels is much more serious than that in the 5 GHz or 2.5 GHz channels [1], [2]. To overcome the high attenuation, beamforming should be used to increase the signal's effective power, while the small wavelength does allow integration of many antenna elements with a small form factor. When it comes to the outdoor environment, highly directional links can be regarded as “pseudowired”

with negligible collision probabilities, as shown in [3], [4]. However, when it comes to the indoor environment, the beamwidth is usually wider than that in outdoor networks due to smaller transmission distances. In this scenario, the pseudowired assumption is no longer applicable, and the interference among neighboring links should be considered [5], [6].

Furthermore, considering the fact that the available spectrum at the mmWave band is large, the fading channel is expected to be frequency selective [7]. Therefore, it is necessary to consider optimizing channel allocation to different links in the network, in order to enhance the overall capacity. On the other hand, due to the fact that signal attenuation is high in mmWave channels, spatial reuse of the mmWave channels should be allowed for multiple links if the mutual interference is tolerable, thus more concurrent transmissions in the network can be achieved and the overall network throughput may be further improved [8].

In this paper we study the problem of supporting multi-user video streaming/downloading in mmWave networks, aiming to minimize the overall video streaming/downloading time for all the links in the mmWave network. We consider the scenario where there are multiple links, multiple channels, and one PicoNet Coordinator (PNC). The PNC is the central coordinator for channel assignment, time slot allocation, and power adaptation for the links. Each link carries a video session from the transmitter to the receiver, and our goal is to minimize the number of time slots required to finish the transmission of all video sessions. Benefited from the high attenuation of the mmWave channel, for each channel, spatial reuse by multiple links can be exploited, as long as they do not cause unacceptable interference to each other. The PNC decides which links to transmit, on which channel, at what power level, and for how long the transmission lasts, so that the time for all links to finish their video transmissions is minimized. For the formulated problem, we developed a column generation based solution method, which greatly reduces the computational complexity and converges quickly to the globally optimal solution.

The main contributions of this paper include

- To the best of our knowledge, this is the first work to study the problem of minimizing the overall scheduling

time of video streaming over mmWave networks, with a rigorous mathematical formulation and analysis.

- The previous works [4]–[6], [9]–[11] on link scheduling in mmWave networks consider only one channel. Here we study the multi-channel case, where frequency diversity at different links are considered, and the corresponding channel allocation problem is solved. Furthermore, unlike prior works [3], [12], we consider the possible co-channel interference that different links cause to each other. Thus our formulated problem and proposed solution are more practical, which can be generalized to other directional networks.
- We formulated an optimization problem that incorporated link scheduling, channel allocation, and power adaptation for streaming videos over mmWave links. Traditional algorithms for the formulated problem has an exponential computational complexity. We develop a column generation based algorithm that iteratively solves the link scheduling, channel allocation, and power adaptation problems, with greatly reduced decision variables and complexity.
- We prove that our proposed algorithm converges to the globally optimal solution, and derive an upper bound for the performance of the proposed algorithm at each iteration. The performance of our proposed algorithm is validated with extensive simulations and comparison with benchmark schemes.

In the remainder of this paper, we present the system model in Section II and the problem formulation in Section III. We develop the column generation based algorithm in Section IV and analyze its performance in Section V. Our simulation study is presented in Section VI. Related works are reviewed in Section VII and Section VIII concludes the paper.

II. SYSTEM MODEL

We consider a mmWave network consisting of multiple channels, multiple links, and one PNC, which is the central coordinator of the network that assigns channels and time slots to the links. Each link contains one transmitter and one receiver, which can directly communicate with each other on a channel, and a link can use at most one channel at any time slot. Different links can spatially reuse a channel as long as they do not cause unbearable interference to each other.

It is challenging to coordinate the transmissions of highly directional links, due to the well-known *deafness* problem. To address this problem, we assume a lower frequency public control channel, such as WiFi, for all nodes in the network [13]. The PNC and nodes exchange network state and control information via the public control channel. Specifically, on the control channel, nodes send their traffic demands and channel updates to the PNC, and the PNC

sends channel and time slot allocation decisions to the nodes [14], [15].

Without loss of generality, we assume that each node works in the half-duplex mode, i.e., a node can either be a transmitter or a receiver at any time slot. An electronically steerable antenna array is equipped at each node, so that each node can beamform at the transmit or receive directions [16]. The co-channel interference among neighboring links is considered in this paper, since the “pseudowired” assumption may not hold true [4], [6], [12]. This is due to the fact that the beamwidth of the directional mmWave transmissions could be wide (e.g., in the indoor environment) [6].

III. PROBLEM FORMULATION

Let \mathcal{L} denote the set of links, and \mathcal{K} the set of channels in the mmWave network. Each link l supports the streaming/downloading of a stored video from the transmitting node (denoted as σ_l) to the receiving node (denoted as ν_l). The traffic demand of each link is the data volume of its video session that needs to be transmitted in the next period of time (e.g., the next Group of Pictures (GOP) period). The video sequence is encoded into High-Priority (HP) data and Low-Priority (LP) to better utilize the interference and loss resilient nature of the video sequences [17]. By optimally assigning the resources to the HP data and LP data, better video quality can be achieved. The quality of reconstructed Medium-Grain Scalable (MGS) video can be modeled as [18]

$$\text{PSNR} = \alpha + \beta \times r_{sum} = \alpha + \beta \times (r_{hp} + r_{lp}), \quad (1)$$

where r_{hp} and r_{lp} are the received data rate of the HP data and LP data, respectively; r_{sum} is the total received data rate, i.e., the sum of r_{hp} and r_{lp} ; α and β are constants associated with the specific video sequence and codec.

According to the Shannon Theorem, to achieve a specific data rate, it is required that the Signal to Interference and Noise Ratio (SINR) at the receiver exceed a threshold corresponding to the data rate, as

$$r = w \times \log_2(1 + \text{SINR}), \quad (2)$$

where w is the bandwidth of allocated spectrum. Given the HP data, for all the links that spatially reuse the same channel, the co-channel SINR at the receiver of each link should exceed a fixed threshold γ_l , which means

$$\text{SINR}_l^k(hp) = \frac{P_l H_l^k}{\rho_l + \sum_{l' \neq l, l' \in \mathcal{L}} I_{l',l}^k} \geq \gamma_l(hp), \forall l \in \mathcal{L}, k \in \mathcal{K}, \quad (3)$$

where P_l is the transmit power at link l , H_l^k is the gain on channel k for link l , $I_{l',l}^k$ denotes the interference caused by link l' on link l on channel k , and ρ_l is the noise power at link l receiver. Denote $\theta(l_1, l_2)$ as the angle offset from the peak channel gain direction from the transmitter of link l_1 to the receiver of link l_2 . Then the potential co-channel

interference caused by link l_1 on link l_2 on channel k can be modeled as $G_{l_1, l_2}^k \Delta(\theta(l_1, l_2))$, where G_{l_1, l_2}^k is the maximum gain on channel k from the transmitter of link l_1 to the receiver of link l_2 , and $\Delta(\theta(l_1, l_2))$ denotes the directional antenna gain as a function of the offset angle $\theta(l_1, l_2)$ [5], [6]. Then we have

$$\begin{aligned} \sum_{l' \neq l, l' \in \mathcal{L}} I_{l', l}^k &= \sum_{l' \neq l, l' \in \mathcal{L}} G_{l', l}^k \Delta(\theta(l', l)) P_{l'} \\ &= \sum_{l' \neq l, l' \in \mathcal{L}} H_{l', l}^k P_{l'}, \end{aligned} \quad (4)$$

where $G_{l', l}^k \Delta(\theta(l', l)) \equiv H_{l', l}^k$. The SINR constraint for the LP video data can be derived and expressed in a similar way, with a lower SINR threshold $\gamma_l(lp)$ for all $l \in \mathcal{L}$.

Without loss of generality, we consider the case that each transmission link can only use up to one channel at a time slot (the multi-channel access case can be handled similarly). Define scheduling index y_l^k as

$$y_l^{k,t} = \begin{cases} 1, & \text{link } l \text{ transmits on channel } k \text{ at time } t \\ 0, & \text{otherwise,} \end{cases} \quad \forall l \in \mathcal{L}, k \in \mathcal{K}, \forall t. \quad (5)$$

Then we have

$$\sum_{k \in \mathcal{K}} y_l^{k,t} \leq 1, \forall l \in \mathcal{L}, \forall t. \quad (6)$$

We define a *schedule* as a set of channel allocation decisions for all the links and all the channels in the network, and a *feasible schedule* is a schedule that the SINR constraint for all the active links, i.e., links that are assigned a channel for transmission in the schedule, are satisfied. Obviously, there may be a huge number of feasible schedules, and different feasible schedules may result in different network throughputs, thus affecting the amount of required time slots to serve the traffic demands of all the links. Let \mathcal{S} be the set of feasible schedules. Our *objective* is to decide which feasible schedule set \mathcal{S} to use, and how many time slots should be assigned for each feasible schedule in \mathcal{S} , so that the overall required time slots to serve the video traffic demands of all the links can be minimized. Note that channel allocation for multiple channels and multiple links are considered when computing the schedule.

As mentioned previously, a feasible schedule should satisfy the SINR constraints on all channels $k \in \mathcal{K}$. Denote the number of time slots allocated for a feasible schedule $s \in \mathcal{S}$ as τ^s . We want to minimize the total transmission time, i.e.,

$$\text{minimize: } \sum_{s \in \mathcal{S}} \tau^s. \quad (7)$$

Note that τ^s can be fractional. Furthermore, only after one schedule is finished then another schedule can be executed. Therefore the schedules will not overlap in any time slot.

Denote the HP data rate of link $l \in \mathcal{L}$ during schedule s as $r_l^s(hp)$, and the LP data rate as $r_l^s(lp)$. To ensure that

the traffic demand of all links sharing channel $k \in \mathcal{K}$ is satisfied, we have

$$\sum_{s \in \mathcal{S}} r_l^s(hp) \tau^s \geq d_l(hp), \forall l \in \mathcal{L} \quad (8)$$

$$\sum_{s \in \mathcal{S}} r_l^s(lp) \tau^s \geq d_l(lp), \forall l \in \mathcal{L}, \quad (9)$$

where $d_l(hp)$ and $d_l(lp)$ are the traffic demand of HP data and LP data, respectively. Note that $d_l(hp)$ and $d_l(lp)$ do not change during the entire scheduling period until the traffic demands of all nodes are served. In fact, if the traffic demand changes, we just need to update the traffic demand at the constraint matrix of the optimization problem P1 (which is given below), and solve the updated problem using the same method. Note that the HP and LP data of a video session may be carried on different channels at each time slot.

We have the following optimization problem.

$$\text{P1: min: } \sum_{s \in \mathcal{S}} \tau^s \quad (10)$$

$$\text{st: } \sum_{s \in \mathcal{S}} r_l^s(hp) \tau^s \geq d_l(hp), \forall l \in \mathcal{L} \quad (11)$$

$$\sum_{s \in \mathcal{S}} r_l^s(lp) \tau^s \geq d_l(lp), \forall l \in \mathcal{L} \quad (12)$$

$$\tau^s \geq 0, \forall s \in \mathcal{S}. \quad (13)$$

Note that the SINR constraints (3) for HP data and LP data are implicitly implied in the above problem in that all feasible schedules in set \mathcal{S} should satisfy the SINR requirement of all active links according to the definition of \mathcal{S} . Solving problem P1 leads to the optimal schedule, which results in the minimum number of time slots to satisfy the video traffic demand of all users under the SINR constraint.

IV. COLUMN GENERATION BASED ALGORITHM

Although problem P1 is in the form of integer linear programming, the main challenge in solving problem P1 is the huge size of the constraint matrix. It takes $\mathcal{O}(2^{|\mathcal{L}|})$, where $|\cdot|$ denotes the number of elements in a set, times of checking constraint (3) to enumerate all the feasible schedules for channel k , for all $k \in \mathcal{K}$, which is computationally expensive. Even if we find all the feasible schedules, since the number of feasible schedules might be so large that the constraint matrix would be too huge for the optimization solver to handle. Therefore, we aim to reduce the number of times of finding the feasible schedules, as well as the size of the constraint matrix for problem P1.

A. Column Generation Based Approach

Column generation is an effective method that can achieve the above two goals [19]–[22]. Column generation decomposes the original problem (problem P1 in our case) into a Master Problem (MP) and a series of Sub-Problems (SP). The MP starts with a subset of columns and variables

of problem P1 and thus is much easier to solve. It also provides a sub-optimal solution to problem P1. The SP is then solved at each iteration to obtain a new column and variable to enter the MP. As the number of columns and variables in the MP increases, the optimal solution to the MP converges to the optimal solution of problem P1. The algorithm terminates until the optimal solution or a sufficiently competitive solution is obtained. Interested readers can refer to [23] for more details.

B. The Master Problem

The Master Problem (MP) in column generation can be initialized as follows. First, we obtain a subset of feasible schedules \mathcal{S}' from set \mathcal{S} , i.e., $\mathcal{S}' \subset \mathcal{S}$, which meets the SINR requirement for each transmission link. Then we calculate the corresponding coefficients r_l^s , for all $s \in \mathcal{S}'$, of the constraint matrix. With \mathcal{S}' , the MP of problem P1 can be expressed as follows.

$$\text{MP: min: } \sum_{s \in \mathcal{S}'} \tau^s \quad (14)$$

$$\text{st: } \sum_{s \in \mathcal{S}'} r_l^s(hp) \tau^s \geq d_l(hp), \forall l \in \mathcal{L} \quad (15)$$

$$\sum_{s \in \mathcal{S}'} r_l^s(lp) \tau^s \geq d_l(lp), \forall l \in \mathcal{L} \quad (16)$$

$$\tau^s \geq 0, \forall s \in \mathcal{S}'. \quad (17)$$

The active transmission links in each feasible schedule are different so that the traffic demand of all links $l \in \mathcal{L}$ will be satisfied. The SINR requirement and traffic demand for each transmission link will be satisfied, which means we have found a subset of feasible schedules and it is a feasible solution to problem P1. Note that the MP only uses a subset of columns (variables/feasible schedules) of problem P1.

A subset of feasible schedules to initialize the MP can be obtained as follows. First, we find a subset of feasible schedules, denoted as $\hat{\mathcal{S}}$, $\hat{\mathcal{S}} \in \mathcal{S}$, such that in each feasible schedule s , $s \in \hat{\mathcal{S}}$, there is only one active link, and this link picks the channel that it has the highest throughput to transmit data (either HP data or LP data). In any two such feasible schedules, either the links are different, or the link transmits HP data in one schedule and transmits LP data in another schedule. We use $\hat{\mathcal{S}}$ to initialize MP. This corresponds to the traditional TDMA schedule.

C. Improving the MP Solution

The optimal Objective Function Value (OFV) of the MP provides an upper bound for the optimal OFV of problem P1, and the MP is much more easier than problem P1 to solve due to a much smaller constraint matrix. Our idea is to iteratively reduce the optimal OFV of the MP by finding a *better* feasible schedule to enter the MP and solve for the optimal OFV at each iteration, until the optimal OFV converges to the optimal OFV of problem P1. The optimality

condition can be checked via the *Most Negative Reduced Cost* of all the feasible schedules [23].

Before doing so, we need to first check whether the current solution to the MP is optimal, i.e., whether the optimal OFV of the MP is already identical to the optimal OFV of problem P1, or if the current solution is not optimal. To check the optimality of the current solution is equivalent to checking whether introducing a new column, i.e., a new feasible schedule in our problem, into the *basis* of the MP, could improve the optimal OFV of the MP. According to the *Simplex Method* in Linear Programming, we can check the *Reduced Cost* of a feasible schedule to see if it can improve the current optimal OFV of the MP [23].

After solving the MP, we can obtain a vector of simplex multipliers [23]

$$(\Lambda(hp), \Lambda(lp)) = (\lambda_l(hp), \lambda_l(lp), \forall l \in \mathcal{L}, \quad (18)$$

where $\Lambda(hp)$ is a $1 \times \|\mathcal{L}\|$ vector with each entry $\lambda_l(hp)$ corresponding to a constraint $\sum_{s \in \mathcal{S}'} r_l^s(hp) \tau^s \geq d_l(hp)$; $\Lambda(lp)$ is the corresponding $1 \times \|\mathcal{L}\|$ vector for LP. The OFV of the MP is an upper bound to the OFV of problem P1.

Then the reduced cost μ^s for any feasible schedule s , i.e., a column of the constraint matrix of the MP, can be expressed as

$$\mu^s = 1 - \sum_{l \in \mathcal{L}} (\lambda_l(hp) r_l^s(hp) + \lambda_l(lp) r_l^s(lp)), \quad (19)$$

where 1 is the coefficient of schedule s in the objective function of the MP.

To find the column and the corresponding variable with the greatest potential to improve the OFV of the MP, we identify the column and the corresponding variable with the most negative reduced cost. Denote $\bar{\mathcal{S}}' = \mathcal{S} \setminus \mathcal{S}'$ as the set of feasible schedules that are not in set \mathcal{S}' . Our objective is to identify a schedule $s^* \in \bar{\mathcal{S}}'$ such that

$$\mu^{s^*} = \arg \min_{s \in \bar{\mathcal{S}}'} \{\mu^s\}, \quad (20)$$

which is equivalent to finding a schedule $s^* \in \bar{\mathcal{S}}'$ such that

$$\begin{aligned} & \sum_{l \in \mathcal{L}} \left(\lambda_l(hp) r_l^{s^*}(hp) + \lambda_l(lp) r_l^{s^*}(lp) \right) \\ & = \arg \max_{s \in \bar{\mathcal{S}}'} \sum_{l \in \mathcal{L}} (\lambda_l(hp) r_l^s(hp) + \lambda_l(lp) r_l^s(lp)). \end{aligned} \quad (21)$$

Denote $\Phi = \mu^{s^*}$ for the ease of later discussions. Once we identify such a schedule s^* , we enter it to the MP and solve the updated MP, to obtain a better solution that achieves a reduced OFV of the MP. Thus the MP solution is continuously improved toward the global optimal solution.

D. Reformulating the SINR Constraint

Considering the fact that a link l can achieve a higher data rate with an SINR significantly greater than its threshold γ , power adaptation is applied in our proposed algorithm

so that each link can optimally tune its transmit power to further improve the throughput of the entire network. For a link l , denote u_l^q as the data rate that can be achieved under an SINR threshold γ_l^q , $1 \leq q \leq Q$. Then the finite set of achievable data rates for link l is $\{u_l^1, u_l^2, \dots, u_l^Q\}$, $\forall l \in \mathcal{L}$ corresponding to the finite SINR threshold set $\{\gamma_l^1, \gamma_l^2, \dots, \gamma_l^Q\}$.

Due to the similarity of the SINR constraints for the HP data and that for the LP data, for simplification we only discuss the HP data case in the following, while the LP data case can be addressed in a similar way. Denote P_{max} as the maximum allowed transmit power for a link. Then the transmit power on link l must follow $0 \leq P_l \leq P_{max}$. If link l transmits on channel k , the SINR constraint for the HP data of link l to transmit at a data rate u_l^q can be expressed as

$$H_l^k P_l \geq \gamma_l^q(hp) \left(\rho_l + \sum_{l' \neq l, l' \in \mathcal{L}} H_{l'l}^k P_{l'} \right), \forall l \in \mathcal{L}, k \in \mathcal{K}. \quad (22)$$

Note that $\gamma_l^q \geq \gamma_l^q(hp)$ for all q .

Denote \mathcal{I}_l^k as the maximum possible interference from all transmitting links, which can be expressed as follows.

$$\mathcal{I}_l^k = \gamma_l^q \left(\rho_l + \sum_{l' \neq l, l' \in \mathcal{L}} H_{l'l}^k P_{max} \right), \forall k \in \mathcal{K}. \quad (23)$$

Define decision variables $x_l^{q,k}(hp)$ and $x_l^{q,k}(lp)$ as follows.

$$x_l^{q,k}(hp) = \begin{cases} 1, & \text{if link } l \text{ transmits HP data at} \\ & \text{rate } u_l^q \text{ on channel } k \\ 0, & \text{otherwise,} \end{cases} \quad (24)$$

$$x_l^{q,k}(lp) = \begin{cases} 1, & \text{if link } l \text{ transmits LP data at} \\ & \text{rate } u_l^q \text{ on channel } k \\ 0, & \text{otherwise.} \end{cases} \quad (25)$$

Then (22) can be rewritten as the following constraint, which considers all links in the network.

$$H_l^k P_l + \mathcal{I}_l^k \left(1 - x_l^{q,k}(hp) \right) \geq \gamma_l^q \left(\rho_l + \sum_{l' \neq l, l' \in \mathcal{L}} H_{l'l}^k P_{max} \right), \forall k \in \mathcal{K}, \quad (26)$$

The reason behind (26) is as follows. If link l transmits HP data at data rate u_l^q , i.e., $x_l^{q,k}(hp) = 1$, then (26) is the same as (22) by eliminating the term $\mathcal{I}_l^k \left(1 - x_l^{q,k}(hp) \right)$.

Otherwise, we have $x_l^{q,k}(hp) = 0$ and the value of \mathcal{I}_l^k can guarantee that (26) is redundant.

E. Solving the Sub-problem

As discussed in the previous section, to improve the OFV of the MP, we need to identify a new column having the most negative reduced cost, which is equivalent to finding

a feasible schedule $s \in \bar{\mathcal{S}}'$ such that $\sum_{l \in \mathcal{L}} (\lambda_l(hp)r_l^s(hp) + \lambda_l(lp)r_l^s(lp))$ is maximized. Then our sub-problem of finding the most negative reduced cost, considering the SINR constraint for a feasible schedule as previously discussed, can be formulated as

$$\begin{aligned} \underline{\text{SP}}: \Psi = \max: & \sum_{k \in \mathcal{K}} \sum_{l \in \mathcal{L}} \lambda_l(hp) \sum_{1 \leq q \leq Q} u_l^q x_l^{q,k}(hp) + \\ & \sum_{k \in \mathcal{K}} \sum_{l \in \mathcal{L}} \lambda_l(lp) \sum_{1 \leq q \leq Q} u_l^q x_l^{q,k}(lp) \end{aligned} \quad (27)$$

s.t.

$$\begin{aligned} & \gamma_l^q \left(\rho_l + \sum_{l' \neq l, l' \in \mathcal{L}} H_{l'l}^k P_{max} \right) x_l^{q,k}(hp) - H_l^k P_l \\ & \leq \gamma_l^q \sum_{l' \neq l, l' \in \mathcal{L}} H_{l'l}^k P_k + \gamma_l^q \sum_{l' \neq l, l' \in \mathcal{L}} H_{l'l}^k P_{max}, \end{aligned} \quad \forall l \in \mathcal{L}, k \in \mathcal{K} \quad (28)$$

$$\begin{aligned} & \gamma_l^q \left(\rho_l + \sum_{l' \neq l, l' \in \mathcal{L}} H_{l'l}^k P_{max} \right) x_l^{q,k}(lp) - H_l^k P_l \\ & \leq \gamma_l^q \sum_{l' \neq l, l' \in \mathcal{L}} H_{l'l}^k P_k + \gamma_l^q \sum_{l' \neq l, l' \in \mathcal{L}} H_{l'l}^k P_{max}, \end{aligned} \quad \forall l \in \mathcal{L}, k \in \mathcal{K} \quad (29)$$

$$\sum_{k \in \mathcal{K}} \sum_{1 \leq q \leq Q} \left(x_l^{q,k}(hp) + x_l^{q,k}(lp) \right) \leq 1, \forall l \in \mathcal{L} \quad (30)$$

$$\begin{aligned} & \sum_{k \in \mathcal{K}} \sum_{1 \leq q \leq Q} \sum_{\sigma_l: l \in \mathcal{L}} \left(x_l^{q,k}(hp) + x_l^{q,k}(lp) \right) + \\ & \sum_{k \in \mathcal{K}} \sum_{1 \leq q \leq Q} \sum_{\nu_l: l \in \mathcal{L}} \left(x_l^{q,k}(hp) + x_l^{q,k}(lp) \right) \leq 1 \end{aligned} \quad (31)$$

$$x_l^{q,k}(hp) \in \{0, 1\}, x_l^{q,k}(lp) \in \{0, 1\}, \quad \forall l \in \mathcal{L}, 1 \leq q \leq Q, k \in \mathcal{K}, \quad (32)$$

$$0 \leq P_l \leq P_{max}, \forall l \in \mathcal{L}. \quad (33)$$

In the above formulation, constraints (28) and (29) enforce that the SINR requirement for the HP data and LP data of each active link be satisfied. Constraint (30) ensures that each link can only transmit either HP data or LP data at a time slot, but not both. In constraint (31), recall that the transmitter node of link l is σ_l and the receiver node of link l is ν_l ; thus (31) indicates that for each node, at most one incident link is activated. Constraint (32) enforces that each link can only either transmit or receive at a time, but not both, since each node operates in the Half-Duplex mode.

V. PERFORMANCE ANALYSIS

A. A Lower Bound on Optimal Performance

At each iteration of the MP computation, the OFV of the MP is updated and becomes more and more closer to the OFV of problem P1. Since our problem is a minimization problem, the OFV of the MP is an upper bound of that

of problem P1. In the following, we show how to derive a lower bound on the OFV of problem P1 at each iteration. Over the iterations, the overall trend is that the upper bound becomes smaller and the lower bound becomes larger, and the upper bound is always greater than the lower bound. After some iterations, the gap between the upper bound and the lower bound will be sufficiently small, indicating that we can terminate our algorithm because we've found an OFV for problem P1 that is close enough to its optimal OFV. Therefore, the lower bound can help us to terminate our algorithm at some early point once we have found a competitive solution, without the need of doing a lot of extra computation to find the exact optimal solution. And of course, we can also continue the iteration until the gap between the upper and lower bounds is reduced to 0, which means we have found the optimal solution for problem P1.

Theorem 1. *At each iteration, let $(\vec{\Lambda}(hp), \vec{\Lambda}(lp)) = (\lambda_l(hp), \lambda_l(lp), \forall l \in \mathcal{L})$, be the dual variable vector obtained from the MP, $(\vec{D}(hp), \vec{D}(lp)) = (d_l(hp), d_l(lp), \forall l \in \mathcal{L})$, as the link demand vector for all links, and Φ as the most reduced cost for all feasible schedules obtained from solving the sub-problem. Then a lower bound for the MP can be expressed as*

$$\begin{aligned} & \frac{1}{1-\Phi} (\vec{\Lambda}(hp) \times \vec{D}(hp) + \vec{\Lambda}(lp) \times \vec{D}(lp)) \quad (34) \\ &= \frac{1}{1-\Phi} \left(\sum_{l \in \mathcal{L}} \lambda_l(hp) d_l(hp) + \sum_{l \in \mathcal{L}} \lambda_l(lp) d_l(lp) \right). \end{aligned}$$

Proof: Denote $\pi = (1, 1, \dots, 1)$ as the coefficient vector of the objective function of the MP, $(\vec{R}(hp), \vec{R}(lp)) = (r_l^s(hp), r_l^s(lp), \forall l \in \mathcal{L})$. Since $(\vec{\Lambda}(hp), \vec{\Lambda}(lp))$ is a dual variable vector obtained from the MP, it is also a feasible solution to the dual problem of the MP (denoted as DMP). According to the relationship between the *primal* program and the *dual* program, it must satisfy

$$(\vec{R}(hp) \quad \vec{R}(lp)) \times \begin{pmatrix} \vec{\Lambda}(hp) \\ \vec{\Lambda}(lp) \end{pmatrix} \leq \pi, \quad (35)$$

which means

$$\begin{aligned} & \vec{R}(hp) \times \vec{\Lambda}(hp) + \vec{R}(lp) \times \vec{\Lambda}(lp) \quad (36) \\ &= \sum_{l \in \mathcal{L}} r_l^s(hp) \lambda_l(hp) + \sum_{l \in \mathcal{L}} r_l^s(lp) \lambda_l(lp) \leq 1, \\ & \forall s \in \bar{\mathcal{S}}' \lambda_l(hp) \geq 0, \lambda_l(lp) \geq 0, \forall l \in \mathcal{L}. \end{aligned}$$

Since Φ is the most reduced cost for all the feasible schedules, and we have $(\vec{\Lambda}(hp), \vec{\Lambda}(lp))$ as the dual variable vector obtained by solving the MP, we have

$$\Phi = \min_{s \in \bar{\mathcal{S}}'} \left(1 - \sum_{l \in \mathcal{L}} r_l^s(hp) \lambda_l(hp) - \sum_{l \in \mathcal{L}} r_l^s(lp) \lambda_l(lp) \right)$$

$$\begin{aligned} & \Rightarrow \sum_{l \in \mathcal{L}} r_l^s(hp) \lambda_l(hp) + \sum_{l \in \mathcal{L}} r_l^s(lp) \lambda_l(lp) \leq 1 - \Phi, \forall s \in \bar{\mathcal{S}}' \\ & \Rightarrow \sum_{l \in \mathcal{L}} r_l^s(hp) \frac{\lambda_l(hp)}{1-\Phi} + \sum_{l \in \mathcal{L}} r_l^s(lp) \frac{\lambda_l(lp)}{1-\Phi} \leq 1, \forall s \in \bar{\mathcal{S}}', \end{aligned}$$

where $\Phi \leq 0$; and $\lambda_l(hp) \geq 0, \lambda_l(lp) \geq 0, \forall l \in \mathcal{L}$.

According to (36), we have that

$$\left(\frac{\lambda_l(hp)}{1-\Phi}, \frac{\lambda_l(lp)}{1-\Phi}, \forall l \in \mathcal{L} \right)$$

is a feasible solution to the DMP. By duality, the corresponding dual LP of a minimization LP is a maximization LP. Therefore, the DMP is a maximization LP, with the following feasible solution.

$$\left(\frac{\vec{\Lambda}(hp)}{1-\Phi}, \frac{\vec{\Lambda}(lp)}{1-\Phi} \right) = \left(\frac{\lambda_l(hp)}{1-\Phi}, \frac{\lambda_l(lp)}{1-\Phi}, \forall l \in \mathcal{L} \right).$$

Let the optimal solution to the DMP be

$$(\vec{\Lambda}^*(hp), \vec{\Lambda}^*(lp)) = (\lambda_l^*(hp), \lambda_l^*(lp), \forall l \in \mathcal{L}).$$

It follows that

$$\begin{aligned} & \left(\frac{\vec{\Lambda}(hp)}{1-\Phi} \quad \frac{\vec{\Lambda}(lp)}{1-\Phi} \right) \times \begin{pmatrix} \vec{D}_l(hp) \\ \vec{D}_l(lp) \end{pmatrix} \\ & \leq (\vec{\Lambda}^*(hp) \quad \vec{\Lambda}^*(lp)) \times \begin{pmatrix} \vec{D}_l(hp) \\ \vec{D}_l(lp) \end{pmatrix} = \Omega, \quad (37) \end{aligned}$$

where Ω is the optimal OFV of the DMP. Due to *Strong Duality*, Ω is also the optimal OFV of the MP. Therefore,

$$\left(\frac{\vec{\Lambda}(hp)}{1-\Phi} \quad \frac{\vec{\Lambda}(lp)}{1-\Phi} \right) \times \begin{pmatrix} \vec{D}_l(hp) \\ \vec{D}_l(lp) \end{pmatrix} \quad (38)$$

is a lower bound for the MP according to (37). \blacksquare

B. Computational Complexity

The MP is a linear optimization problem and is initialized with a small subset of feasible schedules, and only one column is added to the MP at each iteration. We can infer that the MP is easy to solve using traditional linear optimization techniques such as the Simplex Method. The major difficulty of solving for the optimal solution lies in solving the sub-problems, which are Mixed Integer Linear Programming (MILP) problems. However, the size of the sub-problem is small, and the number of decision variables of the MILP sub-problem is $|\mathcal{L}| + Q \cdot |\mathcal{L}| \cdot |\mathcal{K}|$. There are effective solvers, such as the Gurobi MIP solver and the Matlab Intlinprog function (which implements the Branch and Bound algorithm), for solving the MILP. Prior works [24], [25] have effectively solved such kind of problems, especially when the solution space is relatively small.

Table I
SIMULATION PARAMETERS

Parameter	Value
$ \mathcal{L} $	30
$ \mathcal{K} $	5
P_{max}	1 W
ρ	0.1 W
w	200 MHz
Time slot duration	1 s
$G_l^k, \forall l \in \mathcal{L}, k \in \mathcal{K}$	random in $[0, 1]$
$\Delta(\theta(l_1, l_2)), \forall l_1, l_2 \in \mathcal{L}, l_1 \neq l_2$	random in $[0, 1]$

VI. SIMULATION RESULTS

A. Simulation Configuration

In this section we evaluate the performance of our proposed algorithm with Matlab simulations. Here we carry out our simulation based on the H.264 video traces available from [26]. The video traces are High Definition videos with a resolution of 4096×1744 and the frame rate is 24 frames per second. Therefore, by a simple calculation the bit rate for this video sequence is 171.44 MHz. The division of HP and LP video data follows the same approach as in [17].

Our simulation parameters for network configuration [4], [5] are as in Table I unless otherwise specified, and the SINR threshold vector $\Gamma = \{0.1, 0.2, 0.3, 0.4, 0.5\}$. The error bars in the simulation figures represent the 95% confidence interval obtained by repeating each simulation 50 times with different random seeds.

We compare our algorithm with two benchmark schemes. The first benchmark scheme (termed Benchmark 1 in the simulation figures) is proposed in [17], where the authors aim to minimize the distortion of the received video sequence by optimal channel assignment to the HP data and LP data in 60 GHz networks. The second benchmark scheme (termed Benchmark 2) is proposed in [9], [10], where the objective is to minimize the total scheduling time in a 60 GHz network but it does not consider channel allocation. Furthermore, the authors use a heuristic algorithm to solve the minimum scheduling time problem, which results in a sub-optimal solution. Since the channel allocation problem is not considered in the Benchmarks, we combine the channel allocation algorithm proposed in [8] with these two algorithms, for a fair comparison with our proposed algorithm. The basic idea of the channel allocation algorithm proposed in [8] is introduced in Section VII.

B. Simulation Results

Fig. 1 shows the performance comparison of our proposed algorithm and the benchmark algorithms under different network sizes, where the number of links $|\mathcal{L}|$ is varied. The performance metric is the length of scheduling time to satisfy the traffic demands. We can see that the length of scheduling time of all the three algorithms increases as the number of links increases, which is as expected since

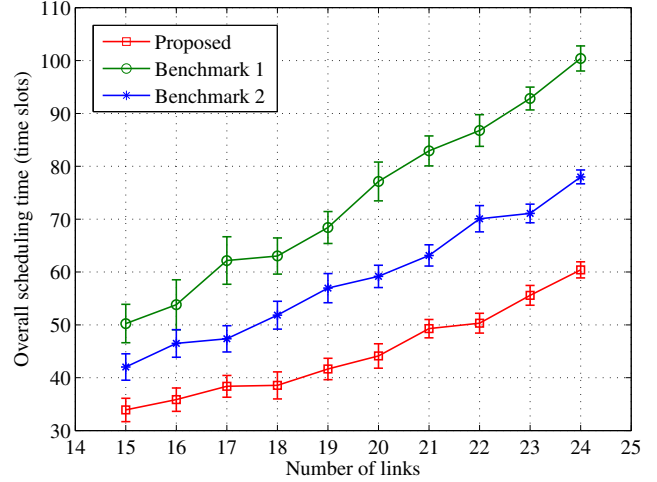


Figure 1. Overall scheduling time versus number of links in the network.

more time slots will be needed to clear the increasing traffic demand. Besides, our proposed algorithm outperforms the benchmarks. The main reason is that, for Benchmark 1, different links may transmit on the same channel. Since there is no coordination for the transmission of multiple links while each link tries to minimize its own distortion, thus they may cause intolerable interference to each other and the data rate for each link will be lower. For Benchmark 2, the authors only consider the minimization of the total scheduling time for all links in a single 60 GHz channel, but does not consider the channel gain diversity among links and the corresponding channel assignment problem for all the links. Thus the schedule would be sub-optimal. Furthermore, Benchmark 2 does not consider transmission power allocation, and thus the links cannot adjust their transmission power when channel conditions varies, and thus further reduces Benchmark 2's throughput performance.

In Fig. 2, we compare the average network delay performance of our proposed algorithm and the benchmark schemes under various link traffic demand. The delay of a link is the duration from the time that the PNC starts to schedule traffic and the time that the traffic demand of the link is served. We can see that as traffic demand is increased, all the three algorithms has a higher average delay, and our proposed algorithm can always achieve a smaller average delay than the benchmark algorithms do. Benchmark 1 does not consider coordinating the concurrent transmissions among multiple links. Therefore different links may select the same channels which have the best channel gain to them while the channels that have lower channel gain are not selected, which may results in low data rate on the selected channels which become crowded. Benchmark 2 does not consider channel diversity among different links and thus its schedules may be sub-optimal. This comparison also demonstrates that channel allocation has a serious negative

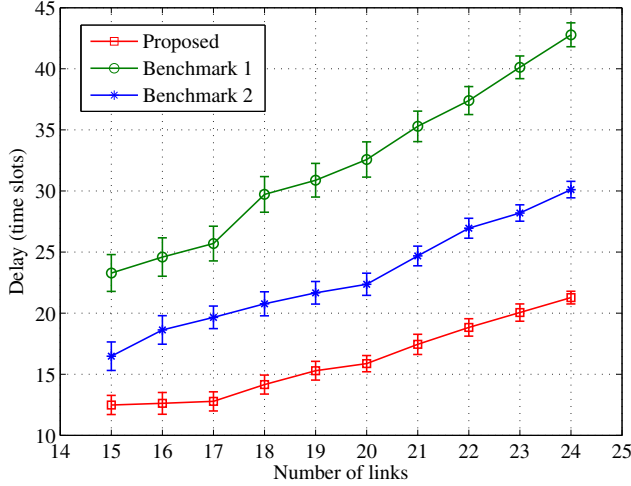


Figure 2. Average delay versus number of links in the network.

effect on delay performance.

The fairness performance comparison of our proposed algorithm and the benchmark algorithms, in terms of average delay of the links, is demonstrated in Fig. 3. The Jains fairness index $f(\{e_1, e_2, \dots\}) = (\sum_{l \in \mathcal{L}} e_l)^2 / (\|\mathcal{L}\| \sum_{l \in \mathcal{L}} e_l^2)$ is adopted here, where e_l is the average delay of all the video sessions transmitted on link l , for all $l \in \mathcal{L}$. A fairness index of 1.0 means the best case, while 0 means the worst case. We can see that the fairness performance of our proposed algorithm is consistently better than that of the two benchmark schemes. The main reason is that since we aim to minimize the total scheduling time, which is dominated by the maximum delay among all links, so our algorithm will try to shorten the maximum delay among all links, which means there is a *minmax* property in our algorithm. Thus our algorithm achieves fairness of delay among the links. The confidence interval has a trend of decreasing, due to an increasing number of samples, i.e., an increasing number of links in the network.

Fig. 4 shows the convergence of the proposed column generation based algorithm. It should be noted that the lower bound as shown in Fig. 4 need not be monotone, and one should therefore maintain the best (highest) value of the lower bounds through the iterations. There are some interesting observations from the two figures.

- The most negative reduced cost Φ has a trend of increasing to 0 over iterations, and the optimal solution is found when Φ reaches 0, which means that we cannot find a schedule that further reducing the total scheduling time. The main reason for the trend is that column generation algorithm chooses the feasible schedule having the most negative reduced cost from the set of candidate feasible schedules to update the MP at each iteration.
- At each iteration, the improvement of the OFV and

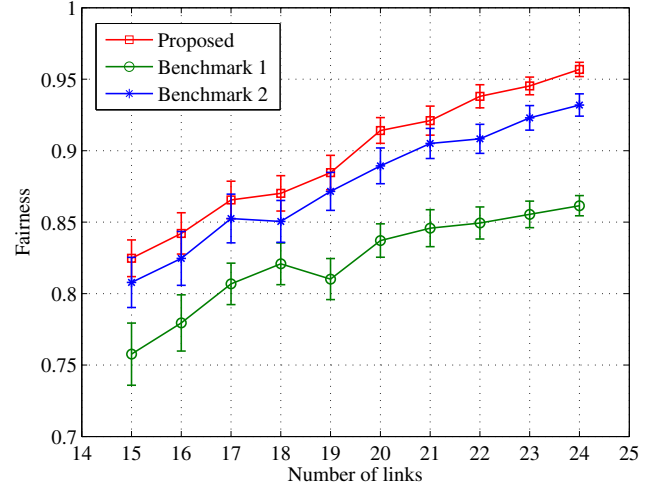


Figure 3. Fairness performance versus number of links in the network.

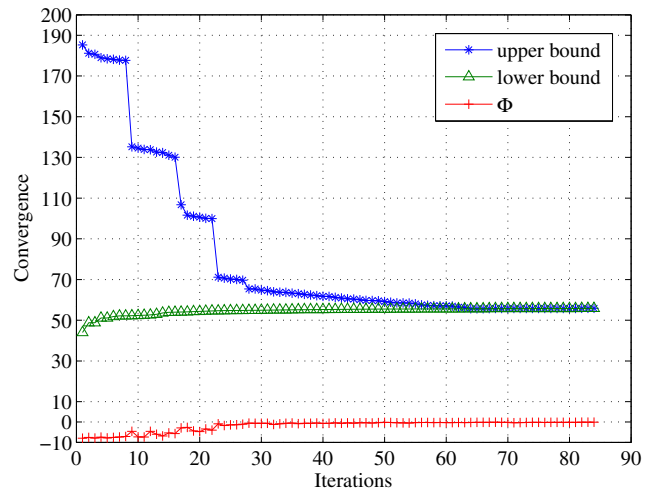


Figure 4. Convergence performance of the column-generation based algorithm.

the most negative reduced cost Φ at this iteration are positively correlated. This is because the most negative reduced cost has the greatest potential to improve the current OFV of the MP.

- The lower bound of the OFV of the MP converges quickly, and is also positively correlated with Φ . From Theorem 1, the lower bound at each iteration is a negative function of Φ . Thus the lower bound will increase as Φ increases from a negative value to 0. Since Φ drops quickly and becomes very close to 0, the lower bound also converges quickly to the optimal value, which is the intersection of the lower bound and the upper bound.

VII. RELATED WORK

In this section we briefly review the key related work on mmWave networks and video streaming. We first examine the interference model in mmWave networks. The authors in [3] claim that due to high signal strength attenuation in the mmWave channel, the interference between different links is negligible and thus a link connecting the transmitting node and receiving node can be regarded as pseudo-wired. On the contrary, the authors in [27] found that the interference between two links is closely related with their relative geo-location and the antenna angle between the links, and thus the concept of exclusive region is proposed. The concept divides the interference between two links into several levels according to their relative geo-location and antenna angle. The authors in [28] conducted measurements at the 38 GHz frequency and found that there are very few unique antenna angles for creating a pseudo-wired link, which suggests that a pseudo-wired link is difficult to find in mmWave networks, especially when the beamwidth is large.

In [5], [6], 60GHz links are modeled as a Partially Observable Markov Decision Process (POMDP), which dynamically switches between two states. The objective is to minimize the overall scheduling time of all the links under the traffic demand constraint. The formulated problem is NP-hard and the authors propose a heuristic algorithm, which tries to maximize the instant network throughput at each time slot. However, performance may not be optimal due to the sub-optimality of the heuristic algorithm and there is no performance bound for the heuristic algorithm. In [4], the authors study the problem of link and relay selection in dual-hop 60 GHz Networks. The dynamic link blockage model adopted in this work is similar to that in [5], [6]. The objective is to find the optimal link and relay selection for each link to minimize the maximum expected delivery time among all links. A decomposition principle is proposed to transform this problem, which is NP-hard, into two sub-problems, one for link selection and the other for relay selection. It is proved that compared with the optimal solution, the proposed algorithm can achieve very competitive performance with a tight performance bound, while the computational complexity is greatly reduced. However, the links are regarded as pseudo-wired in this paper, which means that the interference between different links is negligible, and thus may not be applicable to the scenario where the interference cannot be neglected, such as indoor 60 GHz networks. Besides, the authors consider the single channel case and thus channel allocation is not taken into account in [4].

There are also some interesting work on spatial reuse in mmWave networks. The authors in [8] investigate the problem of channel allocation in 60 GHz indoor WLANs in order to maximize throughput. Two SDMA (Spatial Division Multiple Access) algorithms are proposed, for the single-

channel case and the multiple-channel case, respectively, to exploit the propagation properties so that data rates to end users can be improved. The authors propose that the multiple channels should be aggregated together for transmission in order to further improve the data rate, and it is proposed that links that are at least a certain distance apart can spatially reuse a channel. However, there is no analysis of how large the distance should be and no discussion on how the channel assignment should be optimized in this paper. In [29], the authors developed a scalable heuristic spatial time division multiple access (STDMA) time-slot scheduling algorithm for mmWave network with SDMA through directional antenna system. The main idea of the proposed scheduling algorithm is that all links in the network are assigned a priority, and time slot are allocated to the links based on their respective priority in a descending order. However, the authors only consider the single channel case and only provide a heuristic algorithm for assigning priorities to the links.

In a recent work [30], multiple description coding was used to transmit uncompressed HD video over a mmWave network. However, only a single link with fixed transmit power and a single channel is considered in this work.

VIII. CONCLUSIONS

We developed an efficient algorithm for the problem of resource allocation, including time slot allocation, channel allocation, and power adaptation for transmission links, to support multiple video streaming sessions over mmWave networks. The objective was to minimize the overall scheduling time to finish the video transmissions for all links via joint optimization of channel allocation, time slot allocation, and power allocation. We developed a column generation based method to reformulate the original problem into a new main problem along with a series of sub-problems, with greatly reduced problem size, and thus greatly reduced computational complexity. We proved that optimal solution to the original problem can be obtained by solving the reformulated problem iteratively, and derived a lower bound for the performance of the reformulated problem at each iteration, which will finally converge to the global optimal solution. The proposed scheme is validated with simulations.

ACKNOWLEDGMENT

This work is supported in part by the US NSF under Grant CNS-1320664, and through the Wireless Engineering Research and Education Center (WEREC) at Auburn University.

REFERENCES

- [1] R. C. Daniels and R. W. Heath Jr, "60 GHz wireless communications: emerging requirements and design recommendations," *IEEE Vehi. Technol.*, vol. 2, no. 3, pp. 41–50, 2007.
- [2] S.-K. Yong, P. Xia, and A. Valdes-Garcia, *60GHz technology for Gbps WLAN and WPAN: From theory to practice*. John Wiley & Sons, 2011.

- [3] S. Singh, R. Mudumbai, and U. Madhow, "Interference analysis for highly directional 60-GHz mesh networks: The case for rethinking medium access control," *IEEE/ACM Trans. Netw.*, vol. 19, no. 5, pp. 1513–1527, 2011.
- [4] Z. He and S. Mao, "A decomposition principle for link and relay selection in dual-hop 60 GHz networks," in *Proc. IEEE INFOCOM'16*, San Francisco, CA, Apr. 2016, pp. 1683–1691.
- [5] Z. He, S. Mao, S. Kompella, and A. Swami, "Minimum time length scheduling under blockage and interference in multi-hop mmwave networks," in *Proc. IEEE GLOBECOM 2015*, San Diego, CA, Dec. 2015, pp. 1–7.
- [6] Z. He, S. Mao, and T. Rappaport, "On link scheduling under blockage and interference in 60 GHz ad hoc networks," *IEEE Access Journal*, vol. 3, pp. 1437–1449, Sept. 2015.
- [7] G. Wang, P. Karanjekar, and G. Ascheid, "Beamforming with time-delay compensation for 60 GHz MIMO frequency-selective channels," in *Proc. IEEE PIMRC'15*, Hong Kong, China, Aug./Sept. 2015, pp. 387–391.
- [8] C. Yiu and S. Singh, "SDMA for 60GHz gigabit wireless networks," in *Proc. IEEE ICC'09*, Dresden, Germany, June 2009, pp. 1–6.
- [9] I. K. Son, S. Mao, M. X. Gong, and Y. Li, "On frame-based scheduling for directional mmWave WPANs," in *Proc. IEEE INFOCOM'12*, Orlando, FL, Mar. 2012, pp. 2149–2157.
- [10] I.-K. Son, S. Mao, Y. Li, M. Chen, M. Gong, and T. Rappaport, "Frame-based medium access control for 5G wireless networks," *Springer MONET Journal*, vol. 20, no. 6, pp. 763–772, Dec. 2015.
- [11] G. Yan and D. Liu, "A simple adaptive STDMA scheduling scheme in mmwave wireless networks," in *Proc. ICCAS'13*, vol. 1, Chengdu, China, Nov. 2013, pp. 159–163.
- [12] R. Mudumbai, S. Singh, and U. Madhow, "Medium access control for 60 GHz outdoor mesh networks with highly directional links," in *Proc. IEEE INFOCOM'09*, IEEE, Apr. 2009, pp. 2871–2875.
- [13] H. Park, Y. Kim, T. Song, and S. Pack, "Multiband directional neighbor discovery in self-organized mmwave ad hoc networks," *IEEE Trans. Vehi. Technol.*, vol. 64, no. 3, pp. 1143–1155, 2015.
- [14] H. Chu and P. Xu, "Relay selection with feedback beamforming information for NLoS 60GHz mmwave WLANs/WPANs," in *Proc. IEEE ICC'14*, Sydney, Australia, June 2014, pp. 5514–5519.
- [15] Z. Liu, X. Tao, W. ur Rehman, Z. Xu, and X. Xu, "Opportunistic relay selection and outage performance analysis for 60GHz wireless system," in *Proc. IEEE Globecom Workshops 2013*, Atlanta, GA, Dec. 2013, pp. 328–332.
- [16] L. Li, K. Josiam, and R. Taori, "Feasibility study on full-duplex wireless millimeter-wave systems," in *Proc. IEEE ICASSP'14*, Florence, Italy, May 2014, pp. 2769–2773.
- [17] H. Cui, C. Luo, C. W. Chen, and F. Wu, "Robust uncoded video transmission over wireless fast fading channel," in *Proc. IEEE INFOCOM'14*, Toronto, Canada, Apr./May 2014, pp. 73–81.
- [18] M. Van Der Schaar, S. Krishnamachari, S. Choi, and X. Xu, "Adaptive cross-layer protection strategies for robust scalable video transmission over 802.11 w lans," *IEEE J. sel. areas commun.*, vol. 21, no. 10, pp. 1752–1763, 2003.
- [19] Z. He, S. Mao, and S. Kompella, "A decomposition approach to quality of service driven multi-user video streaming in cellular cognitive radio networks," *IEEE Trans. Wireless Commun.*, vol.15, no.1, pp.728–739, Jan. 2016.
- [20] A. Capone, I. Filippini, and F. Martignon, "Joint routing and scheduling optimization in wireless mesh networks with directional antennas," in *Proc. IEEE ICC 2008*, Beijing, China, May 2008, pp.2951–2957.
- [21] J. El-Najjar, C. Assi, and B. Jaumard, "Joint routing and scheduling in WiMAX-based mesh networks," *IEEE Trans. Wireless Commun.*, vol.9, no.7, pp.2371–2381, July 2010.
- [22] M. Johansson and L. Xiao, "Cross-layer optimization of wireless networks using nonlinear column generation," *IEEE Trans. Wireless Commun.*, vol.5, no.2, pp.435–445, Feb. 2006.
- [23] I. Griva, S. G. Nash, and A. Sofer, *Linear and Nonlinear Optimization*. Siam, 2009.
- [24] G. Zheng, C. Hua, R. Zheng, and Q. Wang, "A robust relay placement framework for 60GHz mmwave wireless personal area networks," in *Proc. IEEE GLOBECOM'13*, Atlanta, GA, Dec. 2013, pp. 4816–4822.
- [25] S. Kompella, J. E. Wieselthier, A. Ephremides, H. D. Sherali, and G. D. Nguyen, "On optimal SINR-based scheduling in multihop wireless networks," *IEEE/ACM Trans. Netw.*, vol. 18, no. 6, pp. 1713–1724, 2010.
- [26] M. Reisslein, "Video traces for network performance evaluation," <http://trace.eas.asu.edu/>.
- [27] L. X. Cai, L. Cai, X. Shen, and J. W. Mark, "REX: a randomized exclusive region based scheduling scheme for mmwave WPANs with directional antenna," *IEEE Trans. Wireless Commun.*, vol. 9, no. 1, pp. 113–121, 2010.
- [28] T. S. Rappaport, E. Ben-Dor, J. N. Murdock, and Y. Qiao, "38 GHz and 60 GHz angle-dependent propagation for cellular & peer-to-peer wireless communications," in *Proc. IEEE ICC'12*, Ottawa, Canada, June 2012, pp. 4568–4573.
- [29] C.-S. Sum, M. A. Rahman, Z. Lan, J. Wang, R. Funada, T. Baykas, H. Harada, and S. Kato, "A scalable heuristic scheduling strategy for 60GHz WPAN STDMA system with directional antennas," in *Proc. IEEE ICC'10*, Cap Town, South Africa, May 2010, pp. 1–6.
- [30] Z. He and S. Mao, "Adaptive multiple description coding and transmission of uncompressed video over 60GHz networks," *ACM Mobile Comput. Commun. Rev. (MC2R)*, vol. 18, no. 1, pp. 14–24, Jan. 2014.